Symmetry-protected single-photon subradiance

Han Cai,[1] Da-Wei Wang,[1] Anatoly A. Svidzinsky,[1] Shi-Yao Zhu,[2] and Marlan O. Scully[1,3,4]
[1]*Texas A&M University, College Station, Texas 77843, USA*
[2]*Beijing Computational Science Research Center, Beijing, China*
[3]*Princeton University, Princeton, New Jersey 08544, USA*
[4]*Baylor University, Waco, Texas 76706, USA*
(Received 22 January 2016; published 2 May 2016)

We study the protection of subradiant states by the symmetry of the atomic distributions in the Dicke limit, in which collective Lamb shifts cannot be neglected. We find that antisymmetric states are subradiant states for distributions with reflection symmetry. Continuous symmetry can also be used to achieve subradiance. This study is relevant to the problem of robust quantum memory with long storage time and fast readout.

DOI: 10.1103/PhysRevA.93.053804

I. INTRODUCTION

Cooperative spontaneous emission (Dicke superradiance [1]) and the cooperative vacuum-induced levels shifts (Lamb shifts [2]) are popular topics in quantum optics. For extended ensembles when the size of the atomic cloud is much larger than the wavelength, the directional emission [3,4] and collective Lamb shift [5] of single-photon superradiance [3,6–13] have attracted much interest. Recently it has been shown [14] that it is possible to use subradiance (the cooperative suppression of spontaneous emission [13]) to store a photon in a small volume for many atomic lifetimes, and later switch the subradiant state to a superradiant state which emits a photon in a small fraction of an atomic lifetime. Such a process has potential applications in, e.g., quantum informatics.

It has been proven that the distribution of the atoms (e.g., periodic or random) in an extended ensemble has a substantial effect on cooperative spontaneous emission [15]. However, the effect of the atomic distribution in the Dicke limit has been studied only a little. Since the distance between atoms is much smaller than the wavelength, one might guess that the distribution of atoms is not important. Here we show that the collective Lamb shift cannot be neglected in general. However, by analyzing the relation between the symmetry of the atomic distribution and cooperative emission, we demonstrate the mitigation of the collective Lamb shift and the symmetry-protected subradiance.

The N-atom sample (size much smaller compared to the transition wavelength λ) excited by a single photon can be described by the Dicke state

$$|+\rangle = \frac{1}{\sqrt{N}} \sum_{j=1}^{N} |j\rangle, \tag{1}$$

where $|j\rangle = |b_1, b_2 \ldots a_j \ldots b_N\rangle$, and a_j (b_j) is the excited (ground) state of the jth atom. Since the size of the atom is much smaller than the wavelength of the coupling field, we could use the dipole approximation. It also allows us to distribute many atoms within one wavelength, which is called the Dicke limit. The probability amplitude of the state (1) decays at the rate $\Gamma_+ = N\gamma$, where 2γ is the single-atom population decay rate. In the "opposite" case, if we neglect Lamb shift, the single-photon subradiance state

$$|-\rangle = \frac{1}{\sqrt{N}} \left(\sum_{j=1}^{N/2} |j\rangle - \sum_{j=N/2+1}^{N} |j\rangle \right) \tag{2}$$

does not decay, i.e., $\Gamma_- = 0$, because of the destructive interference of the atomic transitions. However, when the cooperative Lamb shifts, i.e., the effects of emission and reabsorption of virtual photons, are counted in, it can degrade superradiance [5,16,17]. In single-photon superradiance, this does not overwhelm the collective enhancement of spontaneous emission. This is not so in the case of subradiance, where the collective Lamb shift can now destroy the ability of the atoms to "store" light, i.e., the original subradiant states are no longer necessarily subradiant. For random atomic distribution, since each atom "sees" different neighboring atoms, collective Lamb-shift-type fluctuation-induced dephasing significantly degrades the destructive interference.

II. DICKE LIMIT

We first turn to a more detailed study of the lifetime of the $|-\rangle$ state and the way in which collective Lamb-shift-type fluctuations influence the state evolution. Numerically calculated population decay of the antisymmetric $|-\rangle$ state with and without taking into account virtual transitions are compared in Fig. 1. The Dicke limit ensemble of 100 atoms is randomly distributed along a one-dimensional (1D) line within 0.01λ, where λ is the atomic transition wavelength. Figure 1 shows that collective Lamb shifts Ω_{ij} degrade subradiance of the state $|-\rangle$. Without Lamb shifts, $|-\rangle$ is subradiant. Counting in the Lamb shifts, $|-\rangle$ is composed of both superradiant and subradiant eigenstates. The components of the superradiant eigenstate decay fast, leaving slowly decaying subradiant components.

The simulation is performed in the basis of single-photon eigenstates. The eigenstates decay exponentially, i.e., $|\psi_n(t)\rangle = \sum_j \beta_j e^{-\Lambda_n t/\hbar} |j\rangle$, with Λ_n being the nth complex eigenvalue and β_j being the probability amplitude to find atom j excited. The eigenvalue equations are [11,18]

$$\Lambda_n \beta_i = \gamma \beta_i - i \sum_{i \neq j}^{N} (-\Omega_{ij} + i\gamma_{ij}) \beta_j = \sum_{j}^{N} M_{ij} \beta_j, \tag{3}$$

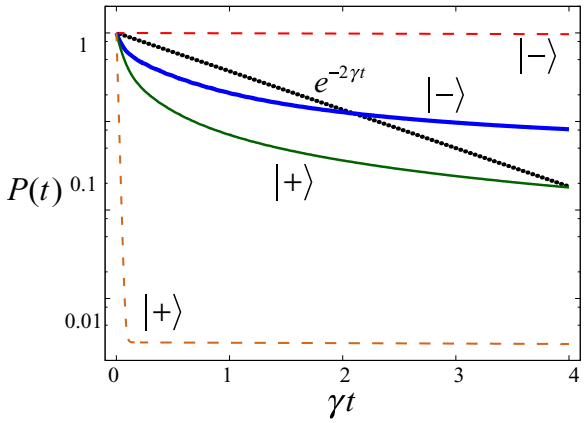

FIG. 1. Probability $P(t) = \langle\Psi(t)|\Psi(t)\rangle$ to find atoms excited as a function of time for atoms initially prepared in the $|+\rangle$ and $|-\rangle$ states. The solid curve takes the cooperative Lamb shift into consideration, causing rapid decay for both $|+\rangle$ and $|-\rangle$. The dashed curve ignores the Lamb shift. For comparison, we also plot single-atom decay curve $e^{-2\gamma t}$ (dotted line).

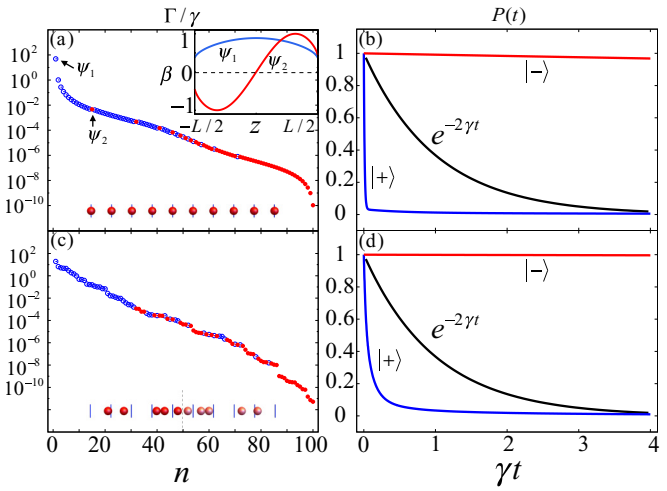

FIG. 2. (a) Distribution of decay rates for eigenstates of an ensemble of 100 atoms regularly placed along a line with spacing between adjacent atoms 0.0001λ. Blue empty dots are symmetric states, while red solid dots are antisymmetric states. Inset: Probability amplitude β_j as a function of the coordinate of the jth atom z_j for the fastest decaying symmetric (blue line) and antisymmetric (red line) states. (b) Population decay of states $|+\rangle$ and $|-\rangle$ as a function of time. The single-atom exponentially decaying curve is shown for comparison. (c),(d) The same as in (a) and (b), but for random spatial distribution of atoms with reflection symmetry.

where $\Omega_{ij} = -\frac{\cos(k_0 r_{ij})}{k_0 r_{ij}}\gamma$, with k_0 the transition wave vector and r_{ij} the distance between atoms i and j, is the collective Lamb shift, $\gamma_{ij} = \frac{\sin(k_0 r_{ij})}{k_0 r_{ij}}\gamma$ is the collective decay rate, and $M_{ij} = \gamma\delta_{ij} + (i\Omega_{ij} + \gamma_{ij})(1-\delta_{ij})$ with δ_{ij} the Kronecker delta function are the elements of the evolution matrix $\mathbf{M}$. This result is based on a scalar radiation field, which can be regarded as the average effect of the vector field [19,20]. We use the scalar field throughout this paper for simplicity. Results for the vector field are shown in the Appendix. There is no essential difference between the results of the scalar and vector fields. Numerically calculating all eigenvalues Λ_n by diagonalization of the matrix $\mathbf{M}$, we obtain $|\Psi(t)\rangle = \sum_n c_n e^{-\Lambda_n t}|\psi_n\rangle$, where $c_n = \langle\psi_n^T|\Psi(0)\rangle$ is the projection of the initial state to the single-photon Dicke-Lamb eigenstate and $\langle\psi_n^T|$ is the transpose of $|\psi_n\rangle$ (since the matrix $\mathbf{M}$ is symmetric instead of Hermitian).

The mitigation of the collective Lamb shifts by arranging the atom distribution in a ring has been found to be useful in maintaining superradiance [21]. If the atoms are distributed randomly, the transition frequencies of atoms are different due to the different environment of each atom and superradiance is destroyed. However, if they are arranged periodically on a ring, all atoms have the same environment and the superradiance is recovered. It sheds light on the importance of the symmetry of the atomic distribution.

Symmetry has long been investigated as a central feature of superradiance [4]. In Dicke's original paper [1], it was noted that the most decaying excited state of the collective atomic distribution must be symmetric since the ground state is symmetric and the Hamiltonian preserves symmetry. The symmetry of the atomic distribution determines the symmetry of the eigenstates. For the sake of simplicity, we take 1D atomic distribution preserving reflection symmetry for an example. We set z along the line of atoms and $z = 0$ as the middle point of the atomic ensemble. The mirror reflection operator π, which transforms $z \to -z$, commutes with the matrix $\mathbf{M}$ for a periodic distribution of atoms, $[\mathbf{M},\pi] = 0$. A nondegenerate eigenstate of $\mathbf{M}$ is also an eigenstate of π [22]. N eigenstates of N atoms excited by a single photon are separated into two groups with opposite eigenvalues of π, i.e., $N/2$ symmetric and $N/2$ antisymmetric states.

In the Dicke limit, the ensemble size is much smaller than the transition wavelength. If we neglect the collective Lamb shifts Ω_{ij} in Eq. (3), we obtain $M_{ij} = \gamma$ for all i and j. In this case, the eigenvalues of $\mathbf{M}$ are $\Lambda_1 = N\gamma$ and all others are equal to zero, i.e., there is one superradiant state and $N-1$ subradiant states [20]. The superradiant eigenstate is the symmetric state $|+\rangle$. Any state orthogonal to this state is subradiant, for example, the antisymmetric state $|-\rangle$. With the presence of Ω_{ij}, $|-\rangle$ is no longer subradiant, as shown in Fig. 1.

We can recover the subradiant nature of the $|-\rangle$ state by rearranging atoms such that their distribution possesses reflection symmetry, i.e., $z_j = -z_{N+1-j}$ and $\pi^\dagger\mathbf{M}\pi = \mathbf{M}$. In Fig. 2(b), we plot the population decay for the periodic distribution of atoms. The decay of $|+\rangle$ is enhanced compared with the case of random distribution, which is consistent with Ref. [21]. On the other hand, the decay of the $|-\rangle$ state is drastically inhibited.

To analyze the reason for this inhibition, we plot β_j for the superradiant state $|\psi_1\rangle$ and for a subradiant state $|\psi_2\rangle$ in the inset of Fig. 2(a). It is clear that the state $|\psi_1\rangle$ is symmetric with respect to the center of the sample. There is only one superradiant state $|\psi_1\rangle$ with decay rate $\sim N\gamma$, as shown in Fig. 2(a). The antisymmetric state $|-\rangle$ is orthogonal to the superradiant state $|\psi_1\rangle$. Because of the Dicke limit, the superradiant state $|\psi_1\rangle$ shown in the inset of Fig. 2(a) is similar to a uniform probability amplitude state $|+\rangle$.

Since reflection symmetry is the key point in the above analysis, it is not necessary for atoms to be periodically

distributed to make the $|-\rangle$ state subradiant. In Fig. 2(c), we allow half of the atoms to be distributed randomly, but in reflection symmetry with the other half. The population decay of the $|-\rangle$ state is still substantially inhibited, as shown in Fig. 2(d). This is because the superradiant state $|\psi_1\rangle$ for random atomic distribution is still symmetric and has no overlap with the $|-\rangle$ state.

Generally, in the Dicke limit, we have one superradiant and $N-1$ subradiant eigenstates. Atomic distribution determines the symmetry of the superradiant state. By preparing atoms in an orthogonal state to this superradiant eigenstate, we can reach subradiance and store the photon. To release the photon, we can coherently change the state to have the same symmetry as the superradiant eigenstate and achieve a rapid readout [14].

III. EXTENDED SAMPLE

We could achieve subradiance in an extended sample as well. For an extended spherical sample, we find [14] approximately decay rates $\Gamma_+^{\vec{k}_0} \cong \gamma[1+\frac{3}{8\pi}\frac{\lambda^2}{A}(N-1)]$ and $\Gamma_-^{\vec{k}_0} \cong \gamma[1-\frac{3}{8\pi}\frac{\lambda^2}{A}]$ for states $|\pm\rangle_{\vec{k}_0} = \sum_{j=1}^{N/2} e^{i\vec{k}_0\cdot\vec{r}_j}|j\rangle \pm \sum_{j=N/2+1}^{N} e^{i\vec{k}_0\cdot\vec{r}_j}|j\rangle$, where λ is the transition wavelength, R is the radius of the atomic cloud, and $A=\pi R^2$ is the cross-section area. The "extra" γ in $\Gamma_+^{\vec{k}_0}$ is not important, as it is small compared to the leading term going as $\frac{3}{8\pi}\frac{\lambda^2}{A}N$. However, the γ term in $\Gamma_-^{\vec{k}_0}$ is important. It seems that for the $|-\rangle_{\vec{k}_0}$ state, the single-atom spontaneous decay rate is a lower decay limit for an extended sample. The good news, however, is that the collective spontaneous decay can also be mitigated by the spatial symmetry of the atomic distribution. In order to calculate the evolution of the atomic system of a dense cloud of volume V, we use an equation with exponential kernel [10],

$$\frac{\partial\beta(t,\mathbf{r})}{\partial t} = i\gamma\int d\mathbf{r}' n(\mathbf{r}')\frac{\exp(ik_0|\mathbf{r}-\mathbf{r}'|)}{k_0|\mathbf{r}-\mathbf{r}'|}\beta(t,\mathbf{r}'), \quad (4)$$

where $\beta(t,\mathbf{r})$ is the probability amplitude to find an atom at position $\mathbf{r}$ excited at time t, and $n(\mathbf{r})$ is the atomic density. Equation (4) is valid in Markovian (local) approximation and is the continuous limit of Eq. (3). Eigenfunctions of Eq. (4) are $\beta(t,\mathbf{r}) = e^{-\Lambda t}\beta(\mathbf{r})$ and the eigenvalues Λ determine the evolution of the atomic system. $\mathrm{Re}(\Lambda)$ yields the state decay rate, while $\mathrm{Im}(\Lambda)$ describes the frequency (Lamb) shift of the collective excitation. The eigenfunction equation for $\beta(\mathbf{r})$ reads

$$-i\gamma\int d\mathbf{r}' n(\mathbf{r}')\frac{\exp(ik_0|\mathbf{r}-\mathbf{r}'|)}{k_0|\mathbf{r}-\mathbf{r}'|}\beta(\mathbf{r}') = \Lambda\beta(\mathbf{r}). \quad (5)$$

We consider an infinitely long cylindrical shell of radius R and use cylindrical coordinates $\mathbf{r}=(\rho,\varphi,z)$. The atomic density is $n(\mathbf{r}) = n_0\delta(\rho-R)/2\pi R$, where n_0 is the number of atoms per unit length of the cylinder. For such geometry, Eq. (5) reads

$$-\frac{i\gamma n_0}{2\pi}\int_0^{2\pi}d\varphi'\int_{-\infty}^{\infty}dz' K(\varphi-\varphi',z-z')\beta(\varphi',z') = \Lambda\beta(\varphi,z), \quad (6)$$

where

$$K(\varphi,z) = \frac{\exp[ik_0\sqrt{2R^2-2R^2\cos\varphi+z^2}]}{k_0\sqrt{2R^2-2R^2\cos\varphi+z^2}}.$$

We look for the solution of Eq. (6) in the form

$$\beta(\varphi,z) = e^{in\varphi}e^{ik_z z}, \quad (7)$$

where n is an integer number and k_z is the wave number of the mode along the cylindrical axis z. Substituting Eq. (7) in Eq. (6), we obtain the following equation for eigenvalues Λ_n:

$$\Lambda_n = -\frac{i\gamma n_0}{2\pi}\int_0^{2\pi}d\varphi'\int_{-\infty}^{\infty}dz' K(\varphi',z')e^{in\varphi'}e^{ik_z z'}. \quad (8)$$

Integrating over z' can be done by using the integral

$$\int_{-\infty}^{\infty}dz'\frac{\exp[ik_0\sqrt{r^2+z'^2}]}{\sqrt{r^2+z'^2}}e^{ik_z z'} = i\pi H_0^{(1)}\big(r\sqrt{k_0^2-k_z^2}\big), \quad (9)$$

where $H_0^{(1)}(x)$ is the Hankel function. Then Eq. (8) reduces to

$$\Lambda_n = \frac{\gamma n_0}{2k_0}\int_0^{2\pi}d\varphi' H_0^{(1)}\big(R\sqrt{2-2\cos\varphi'}\sqrt{k_0^2-k_z^2}\big)e^{in\varphi'}. \quad (10)$$

The integration over φ' can be calculated using

$$\int_0^{2\pi}d\varphi' H_0^{(1)}(a\sqrt{2-2\cos\varphi'})e^{in\varphi'} = 2\pi J_n(a)H_n^{(1)}(a), \quad (11)$$

and Eq. (10) leads to

$$\Lambda_n = \frac{\pi\gamma n_0}{k_0}J_n\big(R\sqrt{k_0^2-k_z^2}\big)H_n^{(1)}\big(R\sqrt{k_0^2-k_z^2}\big). \quad (12)$$

Hankel functions can be written as a combination of the Bessel functions of the first and the second kind as

$$H_n^{(1)}(x) = J_n(x) + iY_n(x), \quad (13)$$

which yields the following answer for the real and imaginary parts of the eigenvalues Λ_n for $k_z \leqslant k_0$:

$$\Gamma_n = \mathrm{Re}(\Lambda_n) = \frac{\pi\gamma n_0}{k_0}J_n^2\big(R\sqrt{k_0^2-k_z^2}\big), \quad (14)$$

$$\Delta_n = \mathrm{Im}(\Lambda_n) = \frac{\pi\gamma n_0}{k_0}J_n\big(R\sqrt{k_0^2-k_z^2}\big)Y_n\big(R\sqrt{k_0^2-k_z^2}\big). \quad (15)$$

Equation (14) shows that the timed Dicke state ($n=0$ and $k_z=k_0$) $\beta(\varphi,z)=e^{ik_0 z}$ has the fastest decay rate, $\mathrm{Re}(\Lambda_{\mathrm{TD}}) = \pi\gamma n_0/k_0$. However, the collective Lamb shift for such state logarithmically diverges since $Y_0(x)\approx(2/\pi)\ln(x/2)$ for small x. For the states with $R\sqrt{k_0^2-k_z^2=A_{nl}}$ where A_{nl} is the lth zero of the Bessel function $J_n(x)$, such as the state $\beta_{n,k_z}(\varphi,z) = e^{in\varphi}e^{iz\sqrt{k_0^2-A_{nl}^2/R^2}} \approx e^{i(k_0-A_{nl}^2/2k_0R^2)z}e^{in\varphi}$, the decay rate and the collective Lamb shift vanish. In Fig. 3, we compare the decay of axially symmetric atomic states for the continuous and discrete distribution of atoms on a cylindrical surface. Namely, we plot the average decay rate $\bar{\Gamma} = -\gamma\ln P(1/\gamma)$ of the state $\beta_{0,k_z}(\phi,z)=e^{ik_z z}$, where $P(t)$ is the probability to find atoms excited, as a function of $R\sqrt{k_0^2-k_z^2-A_{01}}$, where $A_{01}=2.404$ is the first zero of $J_0(x)$. The average decay rate approaches zero when $R\sqrt{k_0^2-k_z^2=A_{01}}$ for a discrete periodic atomic distribution, shown in Fig. 3. This agrees with the analytical result in the continuous limit in Eq. (14) plotted as

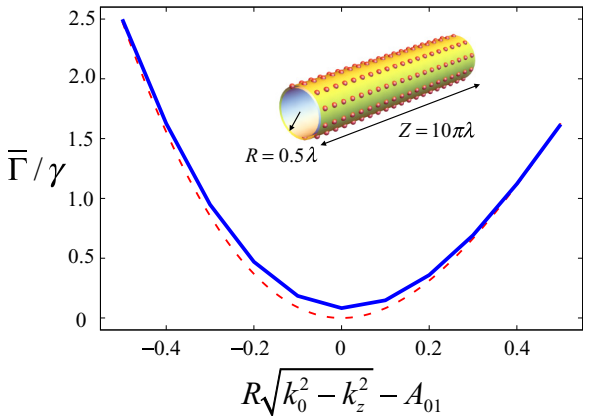

FIG. 3. The solid line shows the average decay rate $\bar{\Gamma}$ of the β_{0,k_z} state for the periodic distribution of atoms on a cylindrical surface sketched on the top. The cylinder consists of 1000 atoms in 100 layers with 10 atoms per each layer. The radius of the cylinder is $R = 0.5\lambda$ and the distance between adjacent layers is $0.1\pi\lambda$. The analytical result (14) for an infinitely long cylindrical shell with $100/\pi\lambda$ atoms per unit length is plotted as a dashed line. The horizontal axis is a deviation of the $R\sqrt{k_0^2 - k_z^2}$ from the root A_{01} of the Bessel function $J_0(x)$. $\bar{\Gamma} = -\gamma \ln[P(1/\gamma)]$ is defined as the average decay rate for a time scale of $1/\gamma$.

a dashed line. Cylindrical atomic distribution can be achieved, e.g., by adhering NV centers or SiV centers on a carbon tube.

IV. CONCLUSION

In summary, we demonstrate that the collective Lamb shifts that are usually thought to destroy subradiance can be mitigated by symmetry. For atomic distributions with mirror symmetry (a discrete symmetry), the antisymmetry states are subradiant, even when half of the atoms are randomly distributed as long as the mirror symmetry is maintained. Periodic distribution with intrinsic mirror symmetry can be realized in ion traps and the subradiant antisymmetry states can be prepared by specially tailored antisymmetric optical modes. In addition, continuous symmetry can also be used to realize subradiance.

ACKNOWLEDGMENTS

We gratefully acknowledge the support of the National Science Foundation Grant No. EEC-0540832 (MIRTHE ERC) and the Robert A. Welch Foundation (Award No. A-1261). H.C. is supported by the Herman F. Heep and Minnie Belle Heep Texas A&M University Endowed Fund held and administered by the Texas A&M University.

APPENDIX: RESULTS WITH VECTOR FIELD

For the sake of simplicity, we use scalar field theory throughout the main text, i.e.,

$$\Omega_{ij} = -\frac{\cos(k_0 r_{ij})}{k_0 r_{ij}}\gamma, \tag{A1}$$

$$\gamma_{ij} = \frac{\sin(k_0 r_{ij})}{k_0 r_{ij}}\gamma. \tag{A2}$$

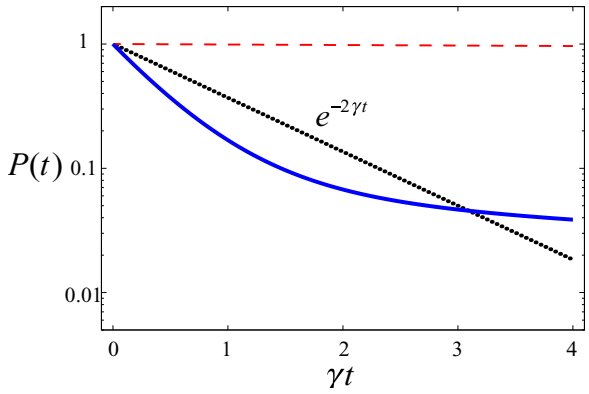

FIG. 4. Results for a vector field with Ω_{ij}^v and γ_{ij}^v. The atomic distribution is the same as Fig. 1 in the main text. Probability $P(t)$ to find atoms excited as a function of time for atoms initially prepared in the $|-\rangle$ state. The solid curve takes the cooperative Lamb shift into consideration. The dashed curve ignores the Lamb shift. For comparison, we also plot single-atom decay curve $e^{-2\gamma t}$ (dotted line).

However, if the polarization of the electromagnetic field is considered, Ω_{ij} and γ_{ij} are [21]

$$\Omega_{ij}^v = \frac{3}{4}\gamma\left\{-P_{ij}\frac{\cos kr_{ij}}{kr_{ij}} + Q_{ij}\left[\frac{\sin kr_{ij}}{(kr_{ij})^2} + \frac{\cos kr_{ij}}{(kr_{ij})^3}\right]\right\}, \tag{A3}$$

$$\Gamma_{ij}^v = \frac{3}{4}\gamma\left\{P_{ij}\frac{\sin kr_{ij}}{kr_{ij}} + Q_{ij}\left[\frac{\cos kr_{ij}}{(kr_{ij})^2} - \frac{\sin kr_{ij}}{(kr_{ij})^3}\right]\right\}, \tag{A4}$$

where factors $P_{ij} = \hat{\mu}_i \cdot \hat{\mu}_j - (\hat{\mu}_i \cdot \hat{r}_{ij})(\hat{\mu}_j \cdot \hat{r}_{ij})$ and $Q_{ij} = \hat{\mu}_i \cdot \hat{\mu}_j - 3(\hat{\mu}_i \cdot \hat{r}_{ij})(\hat{\mu}_j \cdot \hat{r}_{ij})$, $\hat{r}_{ij} = \hat{r}_i - \hat{r}_j$. Here, $\hat{r}_j$ and $\hat{\mu}_j$

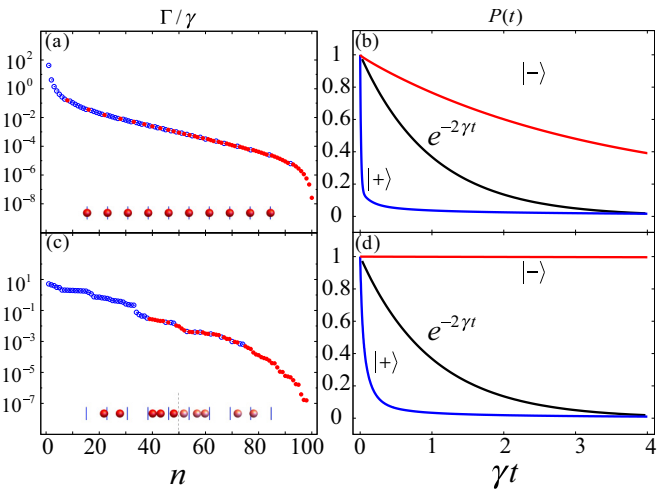

FIG. 5. Eigenvalue distribution and population evolution for a vector field. (a) Distribution of decay rates for eigenstates of an ensemble of 100 atoms regularly placed along a line with spacing between adjacent atoms 0.0006 λ. The blue empty dots are symmetric states, while the red solid dots are antisymmetric states. (b) Population decay of states $|+\rangle$ and $|-\rangle$. A single-atom exponentially decaying curve is shown for comparison. (c),(d) The same as in (a) and (b), but for random distribution of atoms with reflection symmetry.

are the position and dipole of the jth atom, respectively. In Fig. 4, the features of the curve are the same as in Fig. 1. Collective Lamb shift Ω_{ij}^{v} significantly degrades the subradiance of the state $|-\rangle$. In Fig. 5, we could restore subradiance by taking advantage of the symmetry of atomic distribution, which is similar to the result of Fig. 2 with a scalar field.

[1] R. Dicke, Phys. Rev. **93**, 99 (1954).
[2] W. E. Lamb, Jr. and R. C. Retherford, Phys. Rev. **72**, 241 (1947).
[3] M. O. Scully, E. S. Fry, C. H. Raymond Ooi, and K. Wódkiewicz, Phys. Rev. Lett. **96**, 010501 (2006).
[4] A. Crubellier, S. Liberman, and P. Pillet, Opt. Commun. **33**, 143 (1980).
[5] R. Röhlsberger, Fortschr. Phys. **61**, 360 (2013).
[6] C. H. van der Wal, M. D. Eisaman, A. André, R. L. Walsworth, D. F. Phillips, A. S. Zibrov, and M. D. Lukin, Science (NY) **301**, 196 (2003).
[7] A. T. Black, J. K. Thompson, and V. Vuletić, Phys. Rev. Lett. **95**, 133601 (2005).
[8] A. Kuzmich, W. P. Bowen, A. D. Boozer, A. Boca, C. W. Chou, L. M. Duan, and H. J. Kimble, Nature (London) **423**, 731 (2003).
[9] V. Balic, D. A. Braje, P. Kolchin, G. Y. Yin, and S. E. Harris, Phys. Rev. Lett. **94**, 183601 (2005).
[10] A. Svidzinsky and J.-T. Chang, Phys. Rev. A **77**, 043833 (2008).
[11] A. A. Svidzinsky, J.-T. Chang, and M. O. Scully, Phys. Rev. A **81**, 053821 (2010).
[12] D.-W. Wang, R.-B. Liu, S.-Y. Zhu, and M. O. Scully, Phys. Rev. Lett. **114**, 043602 (2015).
[13] A. A. Svidzinsky, X. Zhang, and M. O. Scully, Phys. Rev. A **92**, 013801 (2015).
[14] M. O. Scully, Phys. Rev. Lett. **115**, 243602 (2015).
[15] W. Feng, Y. Li, and S.-Y. Zhu, Phys. Rev. A **89**, 013816 (2014).
[16] R. Friedberg, S. R. Hartmann, and J. T. Manassah, Phys. Rep. **7**, 101 (1973).
[17] M. O. Scully and A. A. Svidzinsky, Science **328**, 1239 (2010).
[18] T. Bienaimé, R. Bachelard, N. Piovella, and R. Kaiser, Fortschr. Phys. **61**, 377 (2013).
[19] G. S. Agarwal, *Quantum Statistical Theories of Spontaneous Emission and Their Relation to Other Approaches* (Springer, New York, 1974).
[20] E. Akkermans, A. Gero, and R. Kaiser, Phys. Rev. Lett. **101**, 103602 (2008).
[21] M. Gross and S. Haroche, Phys. Rep. **93**, 301 (1982).
[22] J. J. Sakurai and J. J. Napolitano, *Modern Quantum Mechanics* (Pearson, London, 2014).